# Suction through Broad Oceanic Gaps

DORON NOF AND SEA HYUCK IM

*Department of Oceanography, The Florida State University, Tallahassee, FL 32306*

(Manuscript received 18 January 1985, in final form 31 May 1985)

ABSTRACT

This paper supplements an earlier article, by Nof and Olson, on the nonlinear flow through broad gaps. In that paper, the steady inviscid transport through a gap located on the left-hand side of a boundary current has been computed. When the gap is located on the right-hand side, instead of the left-hand side, the Nof and Olson solution breaks down because of a singularity at the upstream edge of the gap. The singularity is associated with an infinitely negative pressure resulting from the fact that particles make a "U" turn as they pass through the gap. The present study focuses on these special singular cases.

To avoid the singularity, the use of the integrated *moment of momentum* is adopted because with an appropriate choice of a coordinate system, the contribution of the unknown force (associated with the singularity) to the integrated torque vanishes. This enables one to construct analytical solutions which give the transport through the gap as well as the force associated with the singularity. It is found that a separated current (i.e., a current bounded by a surfacing interface) is always sucked in its entirety into the gap no matter how wide the gap. As in the Nof and Olson study, this result is valid for broad gaps (i.e., gaps whose width is of the order of the deformation radius). For very broad gaps (i.e., much larger than the deformation radius), a perturbation scheme provides an approximate solution which is independent of that derived by the integrated moment of momentum technique. This solution also shows that a separated current is completely sucked into the gap. In view of these solutions, it is concluded that a separated boundary current flowing along a wall with a series of gaps is always sucked *into the first gap* that it encounters.

Application of this theory to the Unimak Pass, which connects the Gulf of Alaska with the Bering Sea, is considered. Using historical data, it is shown that the locations and positions of the currents located near and at the Pass agree with the model predictions.

## 1. Introduction

Recently, attention has been drawn to the flow through passages that, unlike many sea straits, do not have a channel-like structure. Instead, their geometry resembles a gap separating two thin walls so that the fluid spends very little time as it flows from one basin to another (Nof and Olson, 1983, hereafter NO; Toulany and Garrett, 1984).

The steady solutions of NO provide a method for computing the pressure-induced transport through gaps whose width is comparable to the deformation radius.[1] They left, however, a number of important questions unanswered. In particular, one wonders why the NO solution breaks down for passages that are located on the right-hand side of the approaching current. This is an important question because the NO model, as it stands now, is not applicable for passages such as the Unimak Pass which is situated to the right of the southwestward flowing current in the Gulf of Alaska (Fig. 1). The purpose of this study is to find the solution for currents associated with such passages and to further investigate the question of why the NO solution fails for gaps located on the right-hand side.

Although an attempt has been made to make this paper self-contained, frequent references to NO are made and the reader who is interested in the detailed development is advised to look at NO before reading the present paper. The reader who, on the other hand, is merely interested in the results can go directly to the summary.

Consider the following situation as an idealized formulation of our problem (see Fig. 2). Two unbounded basins are separated by an infinitely long wall which contains a gap. The two parts of the wall represent the land masses separating the Gulf of Alaska from the Bering Sea. The wall on the left represents the Aleutian Islands west of the Unimak Pass and the wall on the right represents the Alaska Peninsula. It will become clear later that the fact that the Aleutian Islands chain contains more than one gap will not affect our general results. This may seem, at first, to be unnatural but it is a direct result of the condition that the flow through broad gaps is independent of their width.

The inner basin (Gulf of Alaska) contains two layers of which only the upper is active; the outer basin (Bering Sea) contains, initially, a single motionless layer. Later on, two layers will be present in both basins.

[1] By "comparable" we mean that the gap width can be, say, one third of the deformation radius or twice the deformation radius.

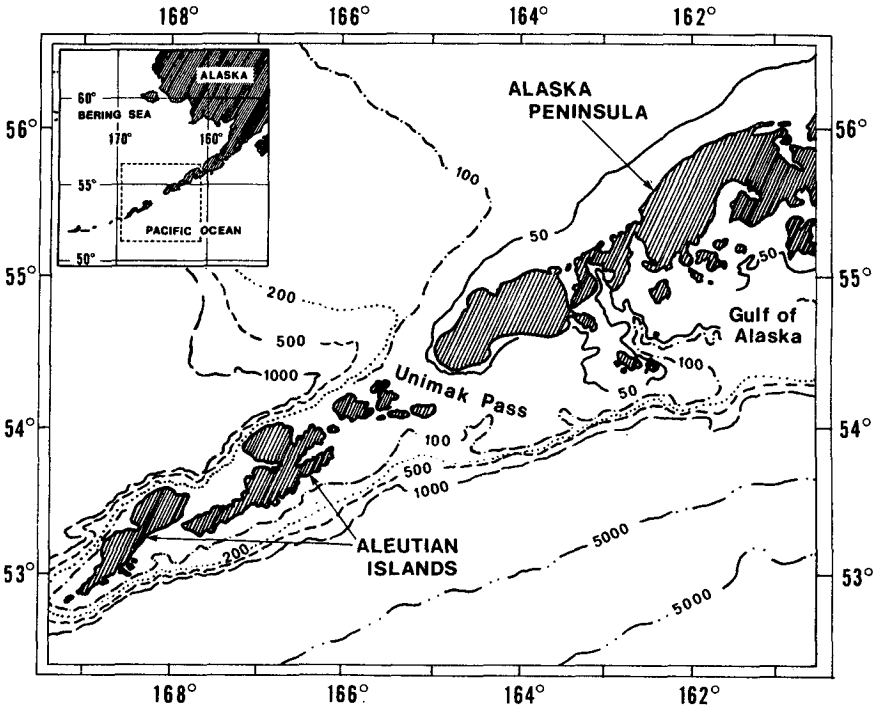


FIG. 1. Location of the Unimak Pass relative to the Aleutian Islands and the Alaska Peninsula (adapted from Canadian Hydrographic Service, 1979). In our model, the Alaska Peninsula and the Aleutian Islands are approximated by long thin walls. Depth contours are given in meters.

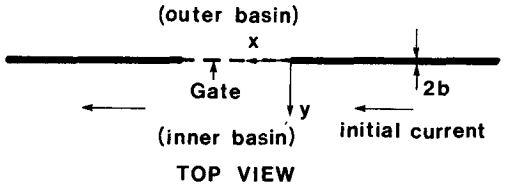


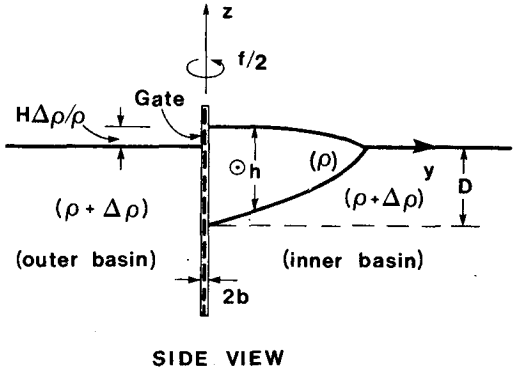


FIG. 2. Schematic diagram of the model's initial conditions. The current flows in the inner basin and the gap is blocked by a gate so that there is no flow from one basin to the other.

Initially, the two basins are separated by a gate extending from the free surface to the interface. The current in the inner basin is flowing in such a way that the gap is located on its right-hand side (looking downstream). Our aim is to determine the steady flow that will be present after the gate is removed and an initial period of adjustment has been completed.

Because of the walls' location and the associated behavior of Kelvin waves (see Fig. 3 and NO), it is expected that the upstream structure will not be altered (see Fig. 4). Under such conditions the situation is similar to Case I of NO with a negative initial current. For this particular case, the NO solution breaks down (see their Fig. 8 with negative flow and their discussion in

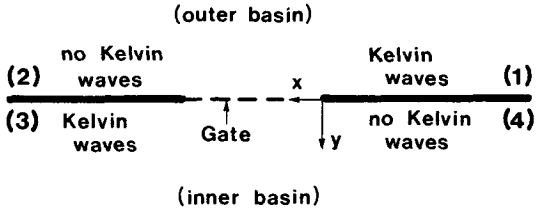


FIG. 3. Schematic diagram of the model's various regions. Since Kelvin waves require a wall on their right-hand side, no Kelvin waves can penetrate into regions (2) and (4), so they remain unaltered. Regions (1) and (3) are the only ones affected by the removal of the gate and the subsequent flow from the inner basin to the outer (cf. Buchwald and Miles, 1974).

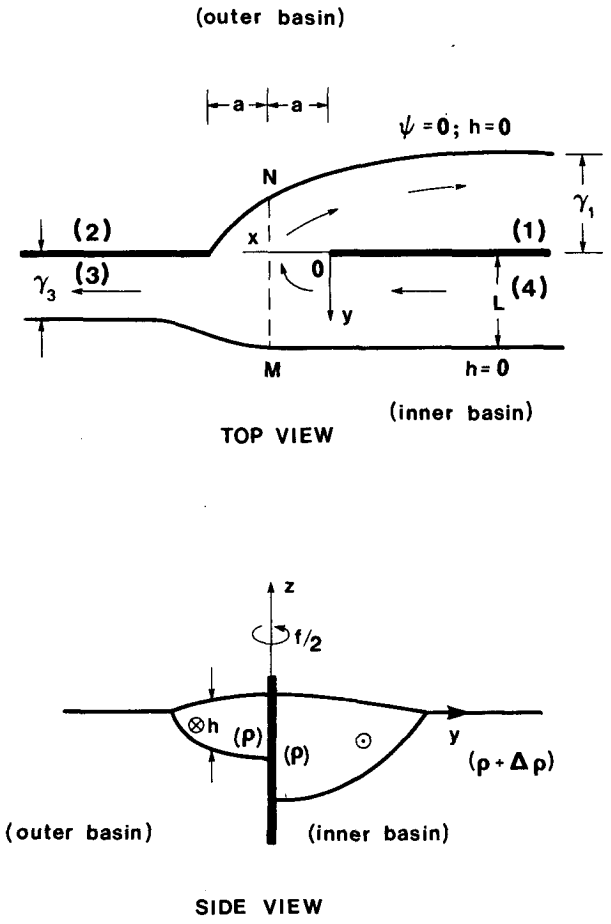


FIG. 4. Schematic diagram of the final steady state for the model under study. The flow in region (4) is the same as the initial flow because no Kelvin waves can reach it. Similarly, region (2) is unaltered and remains stagnant. Note that particles make a sharp "U" turn as they enter the outer basin. In addition, note that the manner in which the penetrating flow separates from the left wall is not important for our analysis as long as the depth (in the outer basin) vanishes along the edge.

the end of Section 3) because the fluid in the vicinity of the right wall turns sharply backward as it enters the outer basin (see Fig. 5).

Under such conditions, the situation in the vicinity of the upstream edge resembles the one occurring in the nonrotating flow around a sharp plate (e.g., Batchelor, 1967, p. 411). As the edge is approached, the distance between adjacent streamlines goes to zero so that the velocity becomes infinite (Fig. 6). Consequently, the Bernoulli function [i.e., $\frac{1}{2}(u^2 + v^2) + p/\rho = B(\psi)$, where $u$ and $v$ are the horizontal two dimensional velocity component, $p$ the pressure, $\rho$ the density and $\psi$ is a streamfunction defined by $\partial\psi/\partial y = -uh$, $\partial\psi/\partial x = vh$ (where $h$ is the upper layer depth)] implies that the pressure is infinitely negative.

As a result, the limit of the integral along the upstream edge,

$$\lim_{b\to 0}\int_{-b}^{b} p\,dy$$

(where $2b$ is the wall's width) *does not vanish* so that there is a force acting in the direction parallel to the walls even though the wall's width is infinitesimal. This additional force, resulting from the singularity of "right-hand side gaps," is not included in the integrated momentum equation used by NO and, consequently, their solution is not valid for such cases. It is important to note that the singularity is represented by an infinitely negative depth at the gap's upstream edge. It will affect all the relations and equations which involve the variables at the upstream edge (e.g., the integrated momentum equation) but it will not affect those relationships which are not directly related to these particular variables (e.g., the integrated continuity equation).

To avoid the effect of the singularity, we shall use the integrated moment of momentum instead of the momentum. It turns out that, for an origin located at the upstream edge of the gap, the contribution of the unknown force to the integrated torque vanishes so that we may obtain the desired information. To verify the results obtained this way, we shall look for some additional computational methods. For this purpose, we shall focus on very broad gaps (i.e., gaps whose width is much larger than the deformation radius but still smaller than the upstream current width) and use a perturbation scheme instead of the integrated moment of momentum. It will be demonstrated that the two methods provide the same answer as should, of course, be the case.

After the solutions are presented and analyzed in detail, the results are compared to the observed transport in the Unimak Pass and the currents in its vicinity. We shall see that, as in the Windward Passage case, the predicted results agree with the location and direction of the observed flows.

This paper is organized as follows: The formulation of the problem is briefly discussed in Section 2; for a detailed discussion the reader is referred to Section 2 of NO. The general solution, which is derived with the aid of the integrated torque, is presented in Section 3, and that derived using the perturbation scheme in Section 4. The applicability of the model to the Unimak Pass is considered in Section 5, and Section 6 summarizes this work.

## 2. Formulation

### *a. General*

Consider again the system shown in Fig. 2; the model is frictionless, hydrostatic and nondiffusive. The origin of our coordinate system is located at the upstream edge of the gap. The $x$ and $y$ axes are oriented across and along the gap (respectively) and the system rotates uniformly at $f/2$ about the $z$ axis. The initial current in the inner basin is flowing at speed $U(y)$; its depth is

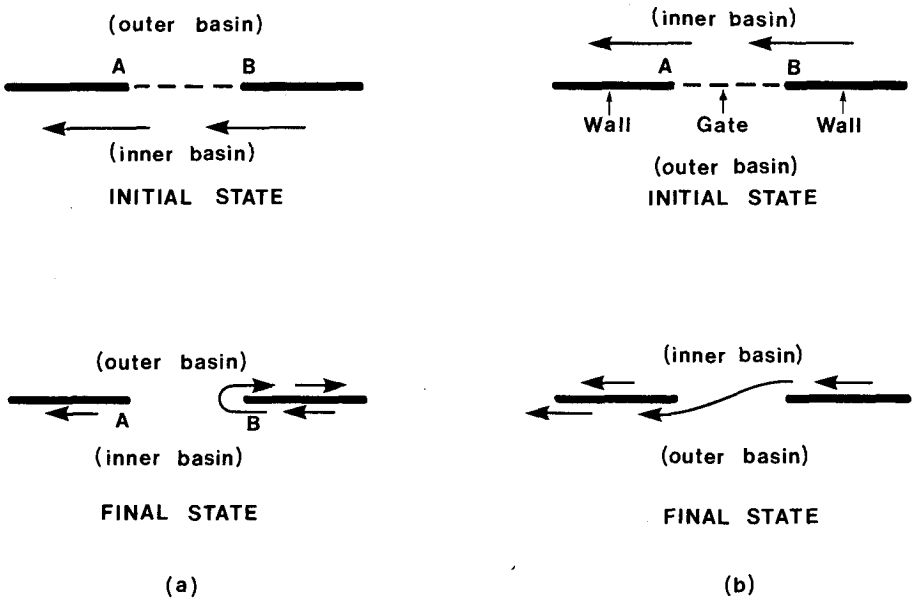


FIG. 5. Schematic diagram of a current with a gap on its right-hand side (left panel), and a current with a gap on its left-hand side (right panel). In (a), the fluid curves sharply backwards as it passes the gap making a sharp "U" turn, whereas in (b) entering particles correspond to an "S" shaped streamline. Situation (b) corresponds to NO whereas situation (a) corresponds to NO with a negative initial flow.

$D(y)$ and its width is $L$ [i.e., $D(L) = 0$]. We define the deformation radius on the basis of the initial current near wall depth ($D_w$); namely, $R_d = (g'D_w)^{1/2}/f$, where $g'$ (the "reduced gravity") is defined by $g\Delta\rho/\rho$. For convenience, we shall take an initial current with uniform potential vorticity $f/D_w$. Hence, we have

$$fU = -g'\frac{\partial D}{\partial y}; \quad -\frac{\partial U}{\partial y} + f = \frac{Df}{D_w}$$

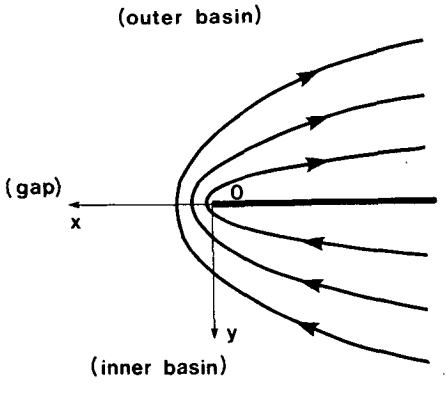


FIG. 6. A diagram of the streamlines corresponding to particles making a "U" turn in the immediate vicinity of a sharp corner. This situation corresponds to a "close-up" of the gap's upstream edge (point B, left panel, Fig. 5). As the edge is approached, the spacing between adjacent streamlines becomes smaller and smaller; when the origin is reached, the distance is infinitesimal so that the velocity becomes infinitely large. Hence, the Bernoulli principle implies that pressure becomes minus infinity.

which give,

$$\left.\begin{aligned} U &= \tfrac{1}{2}U_w(e^{y/R_d} + e^{-y/R_d}), \quad 0 \leqslant y \leqslant L \\ D &= D_w\left[1 - \frac{U_w}{2fR_d}(e^{y/R_d} - e^{-y/R_d})\right], \\ & \qquad\qquad 0 \leqslant y \leqslant L \end{aligned}\right\} \quad (2.1)$$

where $U_w$ is the initial current speed near the wall [i.e., $U_w = U(0)$]. Note that at $y \to \infty$ and $y \to -\infty$, the level of the free surface is identical. The width of the initial current, $L$, corresponds to the location where $D = 0$,

$$L = R_d \ln[(g'D_w)^{1/2}/U_w + (g'D_w/U_w^2 + 1)^{1/2}]. \quad (2.1a)$$

Note that, for many flows of practical interest, the term in the square brackets is considerably larger than unity [i.e., $U_w \ll (g'D_w)^{1/2}$] so that $L$ is, at least, several deformation radii. Furthermore, for a nonseparating current (i.e., a current whose lower interface never strikes the free surface, $D > 0$) the width $L$ goes to infinity even though the decay length scale is the deformation radius. It will become clear later that our choice of uniform potential vorticity is strictly a matter of convenience. Similar results will be found for currents with nonuniform potential vorticity.

It is expected that after the gate is lifted and the initial period of adjustment has been completed, the flow from region 4 (Fig. 4) will split into two branches; one will enter region 1 in the outer basin and the other will continue in the inner basin and enter region 3.

The conditions in regions 2 and 4 will remain identical to those that we have started with because there is no mechanism by which momentum can be transferred to them. Our aim is to determine how the splitting is taking place—namely, to find out how much fluid flows in region 1 and how much fluid enters region 3.

*b. Governing equations and boundary conditions*

Due to conservation of potential vorticity and the fact that away from the gap the flow is one-dimensional we have,

$$-\frac{\partial u_i}{\partial y}+f=h_i f/D_w; \qquad i=1,3 \tag{2.2}$$

$$fu_i=-g'\partial h_i/\partial y; \quad i=1,3 \tag{2.3}$$

where $i=1,3$ corresponds to regions 1 and 3, respectively. The boundary conditions for regions 1 and 3 are,

$$h_1=0; \quad y=-\gamma_1 \tag{2.4}$$

$$\left[\frac{u_1^2}{2}+g'h_1\right]_{y=0}=\frac{U_w^2}{2}+g'D_w \tag{2.5}$$

$$\left[\frac{u_3^2}{2}+g'h_3\right]_{y=0}=\left.\frac{u_1^2}{2}\right|_{y=-\gamma_1} \tag{2.6}$$

$$h_3=0; \quad y=\gamma_3 \tag{2.7}$$

$$u_3^2|_{y=\gamma_3}=U_e^2, \tag{2.8}$$

where $U_e$ is the known velocity along the approaching current edge [i.e., $U_e=U(L)$]. Conditions (2.4) and (2.7) reflect the fact that the interface surfaces (at locations which must be determined as part of the problem) whereas (2.5), (2.6) and (2.8) correspond to conservation of energy along the edges and the walls.

It should be stressed that (2.5), (2.6) and (2.8) correspond to conservation of energy along specific streamlines. Namely, it is assumed here that there are streamlines connecting the upstream region (region 4) with regions 1 and 3. If, for whatever reason, one of the streamlines, which bound the upstream region from left and right, does not connect the regions under discussion then the boundary conditions should be changed accordingly. For example, as pointed out by NO, the unphysical trivial solution for the problem at hand is the one corresponding to no flow through the gap. Clearly, for this case (2.5) cannot be satisfied because there is no flow in region 1 and, consequently, there is no streamline along the right wall in the outer basin. Namely, (2.5) and (2.6) should be replaced by

$$\left[\frac{1}{2}u_3^2+g'h_3\right]_{y=0}=\frac{U_w^2}{2}+g'D_w$$

because the streamline that originates near the wall upstream does not extend beyond the inner basin; it connects the upstream region with the left wall downstream (see Fig. 4).

*c. Constraints*

The first constraint results from continuity (Fig. 4) and, as in NO, can be written in the form,

$$\int_0^L UDdy=\int_0^{-\gamma_1}u_1h_1dy+\int_0^{\gamma_3}u_3h_3dy. \tag{2.9}$$

It will become clear later that, as in NO, this condition is automatically satisfied because we have applied the Bernoulli principle to the edges of the currents so that we have, in fact, stated that the edges are streamlines. Note that since (2.9) does not involve any variables within the gap itself, the singularity has no effect on it.

In contrast to (2.9), the integrated momentum equation will be affected by the singularity because it involves variables within the gap. To illustrate the properties of the singularity, we shall first consider a right wall with a finite width ($2b$) and a smooth round edge (with a radius $r=b$ as shown in Fig. 7). We shall then take the limit (of the desired expressions) as

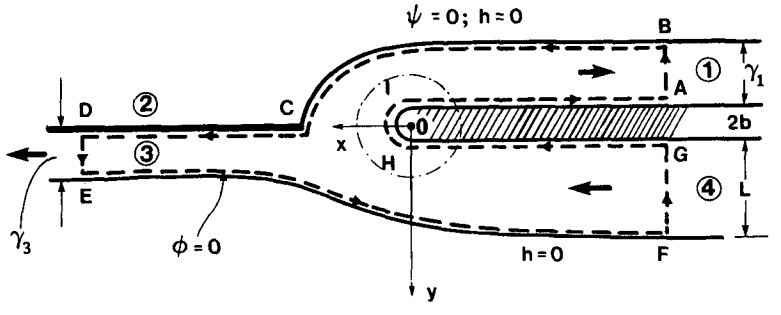


FIG. 7a. Schematic diagram of the integration area for both the momentum equation and the moment of momentum. Because of the singularity at the upstream edge, we initially take the upstream wall to have a finite width, ($2b$) and a smooth round edge. The details of the gap upstream edge (i.e., the area bounded by the dashed dotted circle) are shown in the Fig. 7b.

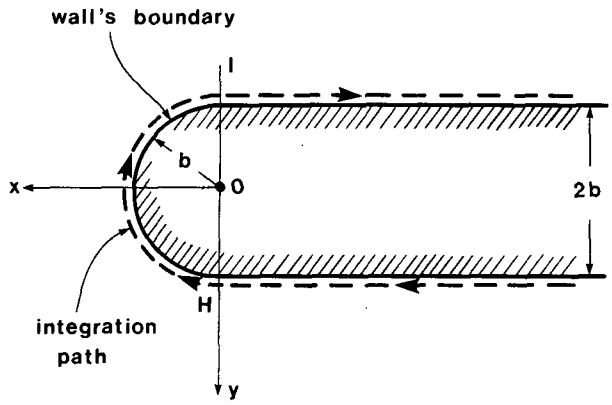


FIG. 7b. A close-up of the region bounded by the dashed dotted circle in Fig. 7a. The round edge position is given by $x^2 + y^2 = b^2$.

$b \to 0$ and return to the original geometry that we have started with (i.e., an infinitesimal right wall as shown in Fig. 4). By following the steps taken by NO, one finds that integration of the $x$ momentum equation over the area shown in Fig. 7 gives,

$$-\oint_\phi huvdx + \oint_\phi hu^2dy - \oint_\phi f\psi dy + \frac{g'}{2}\oint_\phi h^2dy = 0, \quad (2.10)$$

where $\phi$ is the boundary of the integration area (i.e., the dashed line in Fig. 7). Next, we define the streamfunction $\psi$ to be zero along CB, multiply the geostrophic relationships for regions 1, 3 and 4 by their associated depths, and integrate in $y$ to find,

$$f\psi_1 = \tfrac{1}{2}g'h_1^2 \quad (2.11)$$

$$f\psi_3 = \tfrac{1}{2}g'h_3^2 + c_3; \quad f\Psi = \tfrac{1}{2}g'D^2 + C \quad (2.12)$$

where $\Psi$ corresponds to the streamfunction associated with the initial current. Since the left edges of regions 3 and 4 (i.e., the lines where $h_3 = D = 0$) correspond to the same streamline, we immediately find that,

$$c_3 = C. \quad (2.12a)$$

Using these relationships, and noting that along a streamline $udy = vdx$, we can simplify (2.10) to,

$$\int_A^B h_1u_1^2dy + \int_D^E h_3u_3^2dy + \int_F^G DU^2dy + \underbrace{\left[\int_{-b}^{b}(g'h^2/2)dy\right]_{y=(b^2-x^2)^{1/2}}}_{F} = 0 \quad (2.13)$$

where the last integral represents the force exerted on the right wall (i.e., $F$ is the integrated pressure acting on the round edge).

The equation is similar to the integrated momentum equation used by NO except for the last term (which vanishes in the NO case). It is obvious that when the width $b$ is finite, the force $F$ is also finite because the depth along the round edge ($h$) is not zero. *One immediately concludes that for a wall with a finite width we cannot use (2.13) to connect the upstream and downstream fields even if the edge is smooth.* The upstream and downstream fields can be connected with the aid of (2.13) only if $F \to 0$ as $b \to 0$. This was the case in the NO study because in their gaps $h$ is always *finite* along the *edge*. It has been pointed out earlier, however, that for our present case, $h \to -\infty$ as $b \to 0$ so that the integral is finite! Namely, because of the infinitely negative pressure at the upstream edge, the force $F$ does not go to zero when $b$ does.

In summary, we can say that the integrated momentum equation (2.13) does not provide any useful information for our case because, no matter what configuration one is considering, there is always a force acting on the upstream wall. When the wall has a smooth round edge and a finite width, the force simply results from the fact that the depth does not vanish near the upstream edge. When the wall width goes to zero the pressure goes to minus infinity implying that there again is a finite force acting on the wall.

Despite these difficulties with the integrated momentum equation, it is possible to connect the upstream and downstream fields without solving for the flow within the gap itself. We shall shortly see that this can be done by considering the moment of momentum because the unknown force corresponding to the singularity has no torque relative to the origin. To show this, we consider again the integration area shown in Fig. 7. The moment of momentum equation is obtained by considering the cross product of the position vector and the momentum equation; it gives,

$$x\left(u\frac{\partial v}{\partial x} + v\frac{\partial v}{\partial y} + fu\right) - y\left(u\frac{\partial u}{\partial x} + v\frac{\partial u}{\partial y} - fv\right) + xg'\frac{\partial h}{\partial y} - yg'\frac{\partial h}{\partial x} = 0. \quad (2.14)$$

Integration of (2.14) over the volume of the region bounded by $\phi$ and consideration of the continuity equation gives,

$$\iint\left[\frac{\partial}{\partial x}(huvx - hu^2y) + \frac{\partial}{\partial y}(xhv^2 - huvy) + \frac{\partial}{\partial x}(fy\psi) - \frac{\partial}{\partial y}(fx\psi) - \frac{\partial}{\partial x}(g'yh^2/2) + \frac{\partial}{\partial y}(g'xh^2/2)\right]dxdy = 0. \quad (2.15)$$

By using Stokes' theorem, (2.15) can be written as,

$$\oint (huvx - hu^2y + fy\psi - g'yh^2/2)dy - \oint (xhv^2 - huvy - fx\psi + g'xh^2/2)dx = 0. \quad (2.16)$$

This equation can be further simplified by noting that: 1) $h = 0$ along CB and EF (Fig. 7); 2) $udy - vdx = 0$ along a streamline; 3) $\psi = 0$ along DCB; 4) $v = 0$ along AB, DE, FG, GH and AI; and 5) $u = 0$ along HI. Using these relationships and (2.11) and (2.12), one finds,

$$\int_H^I (fy\psi - g'yh^2/2)dy + (fx\psi - g'xh^2/2)dx + \int_I^A (fx\psi - g'xh^2/2)dx - \int_A^B h_1u_1^2ydy - \int_C^D (g'xh^2/2)dx + \int_D^E (-h_3u_3^2y + fy\psi_3 - g'yh_3^2/2)dy + \int_E^F f\psi(ydy - xdx) + \int_F^G (-DU^2y + fy\Psi - g'yD^2/2)dy + \int_G^H (fx\psi - g'xh^2/2)dx = 0 \quad (2.17)$$

where the contribution of the force acting on the round upstream edge to the integrated moment of momentum is represented by the first integral. It is easy to show that this term *is identically zero* for all $b \geq 0$ because the integral is taken along the path $x^2 = b^2 - y^2$; $x \geq 0$, so that $xdx + ydy = 0$. This implies that the force on the round edge has no torque relative to the origin. With this special condition in mind, we can easily take the limit of (2.17) as $b \to 0$. Specifically, because of the vanishing torque, the limit of (2.17) as $b \to 0$ does not involve any new considerations and is essentially trivial. The only difference between the $b \to 0$ case and the finite width case is in the location of points G, H, I and A. By considering (2.12) (2.12a), the geometry of the problem and the fact that $\psi = c_3 = C$ along EF, one finds that (2.17) can be written as,

$$\int_I^A (fx\psi - g'xh^2/2)dx - \int_A^B h_1u_1^2ydy - \frac{1}{2}\int_C^D g'xh^2dx - \int_D^E h_3u_3^2ydy - \int_E^F f\psi xdx - \int_F^G DU^2ydy + \int_G^H (fx\psi - g'xh^2/2)dx = 0 \quad (2.18)$$

where the width $b$ is now zero so that we have returned to our original configuration (Fig. 4). This integrated moment of momentum equation contains the unknowns associated with the far fields (regions 1, 3 and 4) as well as variables in the transition regions (i.e., the areas in the immediate vicinity of the gap). In view of this, we cannot simply eliminate the unknown variables associated with the far fields (i.e., $u_1$, $h_1$, $\gamma_1$, $u_3$, $h_3$, $\gamma_3$) from the governing equations (2.2), (2.3) and (2.18). However, as we shall see in the next section, we can derive the desired solutions simply by inspection. It will become clear shortly, that for downstream solutions that one may guess, one can examine all of the terms in (2.18) and, hence, one can determine whether or not the "guessed" solution is valid. This cannot be done with the integrated momentum (2.13) (and its limit as $b \to 0$) because of the unknown force acting on the upstream edge ($F$).

## 3. Solution

### a. *General solution for regions 1 and 3*

The solutions satisfying (2.2) and (2.3) are

$$u_i = A_ie^{y/R_d} + B_ie^{-y/R_d}; \quad i = 1, 3 \quad (3.1)$$

$$h_i = D_w\left(1 - \frac{A_i}{fR_d}e^{y/R_d} + \frac{B_i}{fR_d}e^{-y/R_d}\right); \quad i = 1, 3 \quad (3.2)$$

where $A_i$ and $B_i$ are constants to be determined from the boundary conditions and constraints. Substitution of (2.4)–(2.8) into (3.1) and (3.2) gives five algebraic equations,

$$1 = \frac{A_1}{fR_d}e^{-\gamma_1/R_d} - \frac{B_1}{fR_d}e^{\gamma_1/R_d} \quad (3.3)$$

$$1 = \frac{A_3}{fR_d}e^{\gamma_3/R_d} - \frac{B_3}{fR_d}e^{-\gamma_3/R_d} \quad (3.4)$$

$$(A_1 + B_1)^2/2 + (g'D_w)^{1/2}(B_1 - A_1) = U_w^2/2 \quad (3.5)$$

$$(A_3 + B_3)^2/2 + (g'D_w)^{1/2}[B_3 - A_3 + (g'D_w)^{1/2}] = (A_1e^{-\gamma_1/R_d} + B_1e^{\gamma_1/R_d})^2/2 \quad (3.6)$$

$$A_3e^{\gamma_3/R_d} + B_3e^{-\gamma_3/R_d} = U_e \quad (3.7)$$

which contain six unknowns $A_1$, $B_1$, $A_3$, $B_3$, $\gamma_1$, $\gamma_3$. An additional condition is, therefore, necessary and, as already mentioned, this *is provided by the integrated moment of momentum.*

For convenience, we rewrite (2.18) in the form,

$$-\frac{1}{2}\int_C^D g'xh^2dx + \int_G^H (fx\psi - g'xh^2/2)dx + \int_I^A (fx\psi - g'xh^2/2)dx - \int_E^F fx\psi dx - \Pi(A_1; A_3; B_1; B_3; \gamma_1; \gamma_3) = 0 \quad (3.8)$$

where the function $\Pi$ is given by,

$$\Pi = \int_A^B h_1 u_1^2 y dy + \int_D^E h_3 u_3^2 y dy + \int_F^G DU^2 y dy \tag{3.9}$$

so that with the aid of (3.1), (3.2) and (2.4)–(2.8) it can be expressed in terms of $A_1$, $A_3$, $B_1$, $B_3$, $\gamma_1$, $\gamma_3$ alone [as already stated in (3.8)]. We shall see shortly that the detailed structure of $\Pi$ (i.e., its structure in terms of our six unknowns) is not important for the present analysis. Note that (3.8) contains two kinds of terms; the first three involve variables associated with the gap and its immediate vicinity whereas $\Pi$, the fourth term, is a function of the far field variables alone.

As pointed out earlier, we cannot, in general, eliminate the first three terms from (3.8) so that we cannot use (3.8) to derive a general algebraic equation for $A_1$, $A_3$, $B_1$, $B_3$, $\gamma_1$, $\gamma_3$. Inspection shows, however, that there are two particular solutions for which the first three terms in (3.8) vanish identically and, in addition, $\Pi = 0$. The first corresponds to the trivial solution—no leakage through the gap (i.e., $u_1 = h_1 = 0$, $u_3 = U$, $h_3 = D$). It is not physically relevant because there is no mechanism that can balance the pressure gradient across the gap. The second particular solution, which (as we shall shortly see) is the relevant solution to the problem, corresponds to the situation where the whole initial current flows into the gap and creates a symmetrical structure (Fig. 8).

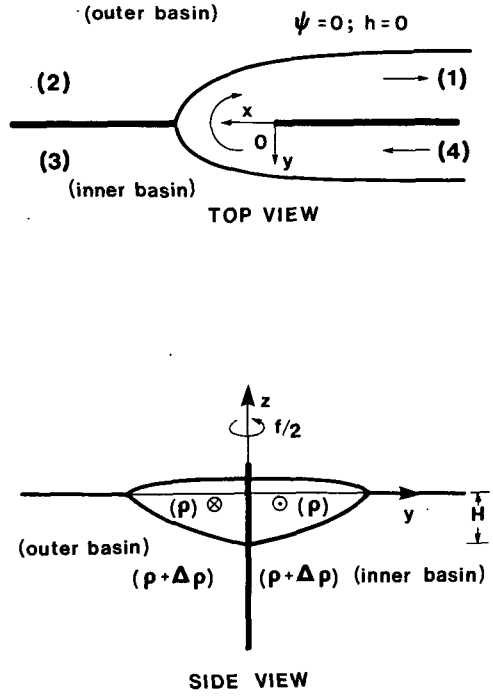


FIG. 8. Schematic diagram of the symmetrical solution. The solution corresponds to a situation where the entire current is sucked into the gap.

For such conditions,

$$u_3 = h_3 = \gamma_3 = 0; \quad u_1 = -U$$

$$= -\frac{1}{2} U_w (e^{y/R_d} + e^{-y/R_d}); \quad \gamma_1 = L \tag{3.10}$$

$$h_1 = D_w \left[ 1 + \frac{U_w}{2fR_d} (e^{y/R_d} - e^{-y/R_d}) \right] = D(-y). \tag{3.11}$$

This solution satisfies all the equations that we have derived [i.e., (3.3)–(3.7) and (3.8)] as well as the appropriate boundary conditions. The latter can be verified by noting that, according to this solution, there is no flow to region 3 so that the streamline originating at the upstream surfacing interface does not reach the left edge of the current in region 3. Instead, it reaches the left edge of the current in region 1. Similarly, there is no streamline connecting the right edge of region 3 with the left edge of region 1. In view of these, (2.6) and (2.8) should be replaced by the single condition,

$$u_1^2|_{y=-\gamma_1} = U_e^2$$

and condition (2.7) degenerates to $\gamma_3 = 0$. It is easy to see that our solution (3.10)–(3.11) satisfies these conditions so that it is a valid solution to our problem as stated above. The advantage and power of the integrated moment of momentum is now clear; with our "guessed" particular solution we could examine all of the terms in (3.8) and (3.9) and, hence, we could state that the integrated torque is conserved. This could have not been done with the integrated momentum because (due to the singularity) any "guessed" flow can, theoretically, satisfy (2.13).

The solution (3.10)–(3.11) enables one to compute the force ($F$) resulting from the singularity. Namely, with the aid of (2.13) we find that,

$$F = \lim_{b \to 0} \int_{-b}^{b} (g'h^2/2) dy|_{y=(b^2-x^2)^{1/2}}$$

$$= -\int_A^B h_1 u_1^2 dy - \int_F^G DU^2 dy \tag{3.12}$$

which, since $u_1 = -U$ and $h_1(y) = D(-y)$, gives

$$F = -2 \int_L^0 DU^2 dy \tag{3.13}$$

where $D$ and $U$ are given by (2.1). Note that this force is identical to that imposed by a separated flow around a wall-like peninsula.

Although our particular solution, obtained by using the integrated moment of momentum, is a valid solution to our problem, we have not really proven that there are no other solutions to the problem. As usual, this is very difficult to do and, therefore, we shall seek some alternative ways of computing the flow to see whether or not a solution different from (3.10)–(3.11) is at all possible. It turns out that the only straightforward alternative to (3.8) is the use of a perturbation

scheme in $\epsilon$, the square of the ratio between the deformation radius and the gap's width. For $\epsilon \ll 1$ (i.e., very broad gaps), we will be able to find solutions independent of the moment of momentum. As should be the case, these solutions agree with our previous predictions (3.10)–(3.11); this analysis is presented in the next section.

## 4. Perturbation analysis

As mentioned above, the purpose of this section is to provide an alternative way for computing the flow through the gap. In contrast to the previous cases where the gap width ($2a$) could take any value (i.e., it could be comparable to the deformation radius or larger than $R_d$), we shall now focus our attention only on very broad gaps (i.e., $a \gg R_d$ but $L > 2a$). We begin by introducing the following nondimensional variables,

$$x^* = x/a;\ y^* = y/R_d;\ h^* = h/D_w;\ R_d = (g'D_w)^{1/2}/f$$
$$u^* = u/(g'D_w)^{1/2};\ v^* = v/(g'D_w)^{1/2}(R_d/a)$$
$$\epsilon = (R_d/a)^2 \ll 1;\ L > 2a. \tag{4.1}$$

Note that $L$, the distance between the wall and the upstream surfacing interface, is taken to be very large even though the length scale in the $y$ direction is $R_d$ (see 2.1a). This may appear, at first, to be unnatural, but it is an appropriate choice because even a nonseparating current (i.e., an infinitely broad current), has a length scale of $R_d$.

It should also be noted that we have assumed here that the current is touching both walls as it is crossing the gap. Under such conditions, the gap width is representative of the current length scale. It is quite possible, however, that, under some conditions, this will not be the case. That is, a current may, perhaps, drastically contract as it flows around the upstream edge and may, therefore, be separated from the downstream edge. This point will be further discussed in the end of the section.

In terms of the nondimensional variables defined by (4.1), the momentum equations are

$$u^* \frac{\partial u^*}{\partial x^*} + v^* \frac{\partial u^*}{\partial y^*} - v^* = -\frac{\partial h^*}{\partial x^*} \tag{4.2}$$

$$\epsilon\left(u^* \frac{\partial v^*}{\partial x^*} + v^* \frac{\partial v^*}{\partial y^*}\right) + u^* = -\frac{\partial h^*}{\partial y^*}. \tag{4.3}$$

It is further assumed that $u^*$, $v^*$, and $h^*$ possess power series expansions in $\epsilon$, e.g.,

$$u^* = u^{(0)} + \epsilon u^{(1)} + \epsilon^2 u^{(2)} + \cdots. \tag{4.4}$$

For such expansions, the zeroth order balances are

$$u^{(0)} \frac{\partial u^{(0)}}{\partial x^*} + v^{(0)} \frac{\partial u^{(0)}}{\partial y^*} - v^{(0)} = -\frac{\partial h^{(0)}}{\partial x^*} \tag{4.5}$$

$$u^{(0)} = -\frac{\partial h^{(0)}}{\partial y^*}. \tag{4.6}$$

Multiplication of (4.6) by $h^{(0)}$ and integration in $y$ gives

$$\psi^{(0)} = h^{(0)2}/2 + c \tag{4.7}$$

where $\psi$ is the streamfunction and,

$$\psi^* = \psi^{(0)} + \epsilon\psi^{(1)} + \cdots. \tag{4.8}$$

It will become clear shortly that, although (4.7) is the familiar formula for the geostrophic transport, the conditions under which it is valid are not at all common. In addition, it will become clear that it could not have been derived without performing the detailed perturbation analysis.

As before, we define $\psi$ to be zero along the line where $h = 0$ in the outer basin so that $\psi^{(0)} = 0$ where $h^{(0)} = 0$ and, consequently, $c = 0$. Hence, we may write (4.7) in a dimensional form,

$$\psi = g'h^2/2f + O\left[\left(\frac{R_d}{a}\right)^2 g'h^2/2f\right]. \tag{4.9}$$

Equation (4.9) states that to $O(\epsilon)$ the transport within the gap is geostrophic. It is important to note, however, that, in contrast to channel-like straits, the flow is *ageostrophic in the cross-strait direction and geostrophic in the long-strait direction.* In other words, had the two basins been connected by a channel rather than a gap, then the geostrophic balance would have been present in the $x$ direction rather than the $y$ direction. Before considering the detailed application of (4.9) to our model, it is instructive to point out that, according to (4.9), the transport between two points is independent of the depth distribution; the transport depends only on the depth at the two end points.

Let us suppose now that we do not know the answer obtained in Section 3 (i.e., the suction of the entire separated current through the gap), but we do know that the gap is larger than the deformation radius. Application of (4.9) to cross section MN (Fig. 4) implies that to $O(\epsilon)$ there is no net transport through MN because the depths at the two end points vanish. This means that all the flow crossing MN from right to left must cross MN again in the reverse direction. It implies that to $O(\epsilon)$ there is no flow in region 3 so that the whole current is sucked into the gap. This result is identical to that obtained in Section 3 by using the integrated moment of momentum. It should be remembered, however, that the integrated torque approach is valid for any gap whose width is not very small compared to $R_d$, whereas the perturbation analysis is only valid for gaps with $a \gg R_d$.

Finally, it should be stressed that in adopting the perturbation scheme we have, in fact, assumed that the width of the gap is representative of the flow within the gap. This is plausible because the upstream width $L$ is larger than $2a$. It may not, however, be the case because the flow may drastically converge as it is going around the upstream edge so that the actual length scale along the $x$ axis may be smaller than $2a$. Under such conditions, the flow is separated from the down-

stream wall and does not even "know" that it exists. Without performing a detailed analysis of the nonlinear flow around the corner, which is beyond the scope of this study, it is impossible to tell which situation will actually occur. It should be remembered, however, that, whether or not the current touches the downstream wall, both situations correspond to a current that is entirely sucked into the outer basin. This general property is the main point of our paper.

## 5. Application to the Unimak Pass

Two general comments should be made before considering the detailed application of our model to the Unimak Pass. First, it is possible to show that the symmetrical solution, obtained in Section 3 with the aid of the integrated torque, is also valid for sloping bottoms provided that the associated depths are symmetrical with respect to the $x$ axis and that the lower layer can still be taken to be motionless. Second, it is recalled that the difference between the integrated torque (2.18) for an infinitesimal wall ($b \to 0$) and the torque associated with a finite width wall is merely in the positions of points F G H I A B (see Fig. 7). Hence, it is easy to show that *the symmetrical solution for a separated current is also adequate when the wall widths are not infinitesimal.* With the aid of this additional information, we shall now consider the application of our symmetrical solution to the Unimak Pass.

The Unimak Pass is the easternmost passage in the Aleutian Islands; it connects the Bering Sea with the Gulf of Alaska (Fig. 1). The Pass has an average depth of ~55 m and at its narrowest point it is ~20 km wide. A light coastal current approaches the Pass from the east (cf. Schumacher and Reed, 1980; Reed and Schumacher, 1981; Royer, 1982; Schumacher *et al.*, 1982). The transport of this coastal current immediately to the east of the Unimak Pass is unknown but much further to the east, near 150°W, the transport is estimated to be ~O($10^5$ m$^3$ s$^{-1}$) (e.g., see Schumacher *et al.*, 1982).

At the eastward entrance to the Pass, the current essentially behaves as a separated current, i.e., the isopycnals intersects the surface (see Fig. 9). Schumacher *et al.* (1982) estimate that, at this location, the average

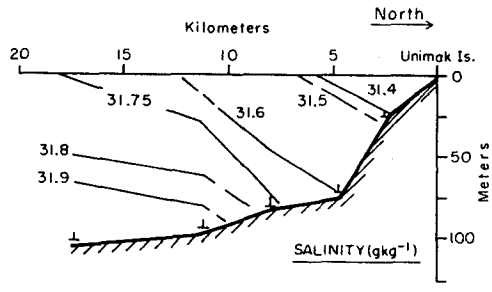


FIG. 9. The salinity structure as derived from a cross-section along 164°30′ (adapted from Schumacher *et al.*, 1982).

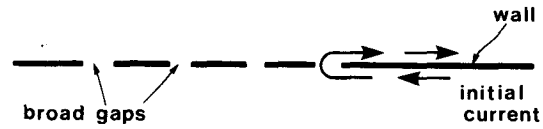


FIG. 10. Schematic diagram of a current approaching a series of broad gaps on its right side. According to our model prediction, the entire current will be sucked into the first gap that it encounters.

transport can be up to ~$0.25 \times 10^6$ m$^3$ s$^{-1}$. The density difference between the upper portion of the water on the shelf and the deep water is roughly two parts per thousand (e.g., see Fig. 6 in Schumacher *et al.*, 1982) and the upper layer depth is approximately 60 meters so that with a Coriolis parameter of $1.2 \times 10^{-4}$ s$^{-1}$ we have a deformation radius of roughly ten kilometers. Since the width of the Pass at its narrowest point is about 20 km, the Pass can be categorized as "moderately broad" [i.e., $a \sim O(R_d)$].

With an upstream near-wall depth ($D_w$) of ~60 meters, the geostrophic transport ($g'D_w^2/2f$) is roughly one third of a sverdrup (i.e., ~$30 \times 10^4$ m$^3$ s$^{-1}$) which is of the same order as the transport suggested by Schumacher *et al.* (1982). For a near wall velocity of about 5 cm s$^{-1}$ we find that the width of the upstream current, $L$, is about forty kilometers which is twice the gap width. It is now recalled that (i) according to our model, the coastal current flowing along the Alaska Peninsula should enter the first gap that it encounters and (ii) the current should be entirely sucked into the gap as shown schematically in Fig. 10. The Unimak Pass is certainly the first gap that the coastal current in the Gulf of Alaska encounters and it is, therefore, expected that the whole current will be sucked in. Indeed, there are numerous observations which support this predicted behavior (see Im, 1985). Among these observations are those of Takenouti and Ohtani (1974), Schumacher *et al.* (1982) and Schumacher and Kinder (1983).

In order to thoroughly examine the question of which water approaches the pass, which water leaks to the Bering Sea and whether any coastal water (associated with the coastal current) continues to flow along the left side of the Aleutian Islands, all the salinity data sets which are available today have been combined and analyzed. Data from the NODC archives for the period 1929–74 (total of 1347 stations) and from NOAA[2] for the period 1975–83 (total of 1388 stations) were used.

Figure 11 shows the simple mean values of the salinity in the region. The salinity contours were drawn (by eye) from the raw (unsmoothed) data. Note that waters with a salinity less than 31.7‰ are found south and north of the Alaska Peninsula. This strongly suggests a flow pattern similar to that predicted by our model. As the model predicts, no coastal flow continues along the Aleutian Islands; namely, the whole current is sucked into the Pass.

[2] Courtesy of J. Schumacher, PMEL.

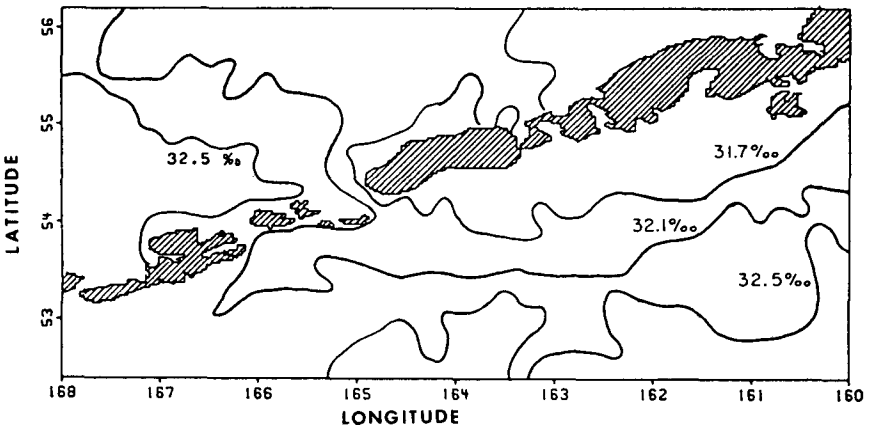


FIG. 11. Salinity contours at 20 m in the vicinity of the Unimak Pass. Note that the Unimak Pass is centered around 54°20'N, 165°W. In addition, note that the contours display a flow structure that is rather similar to that predicted by our model (Figs. 8, 10).

Before completing our present discussion, it is appropriate to point out that our model is applicable to the Unimak Pass even though the Unimak Island is not an infinitesimal wall,[3] and even though the actual bottom is sloped. This results from the fact that, as mentioned earlier in the beginning of this section, our model results can easily be extended to such cases provided that the actual barrier shape, as well as the topography, are approximately symmetrical relative to the $x$ axis.

## 6. Summary and conclusions

This study extends the work of Nof and Olson (1983) to gaps located on the right-hand side of an approaching current. For such gaps the Nof and Olson theory fails because of a singularity at the upstream edge of the gap. The singularity results from the fact that the particles make a "U" turn as they enter the outer basin and, therefore, the streamlines curve sharply backwards near the upstream edge. Consequently, an infinitely low pressure develops at the edge and this gives rise to a force acting on the wall even though the wall width is infinitesimal. The singularity is avoided by taking the following approaches.

First, we consider the integrated moment of momentum instead of the momentum equation because the force resulting from the singularity does not have any torque relative to the gap edge. Second, we use a perturbation scheme in $\epsilon$, the square of the ratio between the deformation radius ($R_d$) and the gap width ($a$), to derive the desired solutions. These two different approaches enable one to construct solutions for both moderately broad gaps [i.e., $a \sim O(R_d)$] and very broad gaps (i.e., $a \gg R_d$). The solutions and their implications can be summarized as follows:

1) A separated boundary current (i.e., a current bounded by a wall on the right and a surfacing interface on the left) encountering a broad gap on its right-hand side is sucked in its entirely into the adjacent basin *no matter how broad the gap.* This result is quite different from that which would be obtained when the gap is located on the left-hand side. As pointed out by NO, under such conditions, only a portion of the current penetrates into the outer basin. Note that our result for "right-side gaps" is valid for both moderately broad gaps and very broad gaps. For currents that squeeze through very narrow gaps ($a \ll R_d$) the theory is not valid because the flow may become "supercritical" within the gap and, as a result, the system may include shock waves and hydraulic jumps (see, for example, Nof, 1984).

2) A separated boundary current flowing along a wall with a series of broad gaps will enter only the first gap. No current will be present downstream and there will be no exchange of water through the remaining gaps.

Qualitative application of this theory to the Unimak Pass is considered in detail. For this case our model predicts that when the southwestward flowing coastal current of the Gulf of Alaska reaches the Unimak Pass, it is sucked into the Pass and then continues northeastward along the coast of the Alaska Peninsula in the Bering Sea. These results agree with the observed currents and salinity structure in the area.

*Acknowledgments.* We thank J. Schumacher for useful conversations and for providing the salinity data for the region. This study was supported by the Office of Naval Research contract N00014-82-C-0404.

[3] The island is, in fact, as wide as the Rossby radius.

REFERENCES

Batchelor, G. K., 1967: *An Introduction to Fluid Dynamics.* Cambridge University Press, 615 pp.

Buchwald, V. T., and J. W. Miles, 1974: Kelvin-wave diffraction by a gap. *Aust. Math. Soc. J.*, **17**, 29–34.

Canadian Hydrographic Service, 1979: *General Bathymetric Chart of the Oceans.* No. 5.03, Ottawa, Canada.

Im, S. H., 1985: Suction through broad oceanic gaps with application to Unimak Pass. M.S. thesis, Florida State University, 67 pp.

Nof, D., 1984: Shock waves in currents and outflows. *J. Phys. Oceanogr.*, **14**, 1683–1702.

——, and D. B. Olson, 1983: On the flow through broad gaps with application to the Windward Passage. *J. Phys. Oceanogr.*, **13**, 1940–1956.

Reed, R. K., and J. D. Schumacher, 1981: Sea level variations in relation to coastal flow around the Gulf of Alaska. *J. Geophys. Res.*, **86**, 6543–6546.

Royer, T. C., 1982: Coastal fresh water discharge in the Northeast Pacific. *J. Geophys. Res.*, **87**, 2017–2021.

Schumacher, J. D., and R. K. Reed, 1980: Coastal flow in the northwest Gulf of Alaska: The Kenai Current. *J. Geophys. Res.*, **85**, 6680–6688.

——, and T. H. Kinder, 1983: Low frequency current regimes over the Bering Sea shelf. *J. Phys. Oceanogr.*, **13**, 607–623.

——, C. A. Pearson and J. E. Overland, 1982: On exchange of water between the Gulf of Alaska and the Bering Sea through Unimak Pass. *J. Geophys. Res.*, **87**, 5785–5795.

Takenouti, A. Y., and K. Ohtani, 1974: Currents and water masses in the Bering Sea: A review of Japanese work. *Oceanography of the Bering Sea,* D. W. Hood and E. J. Kelly, Eds., Institute of Marine Sciences, University of Alaska, 39–57.

Toulany, B., and C. Garrett, 1984: Geostrophic control of fluctuating barotropic flow through straits. *J. Phys. Oceanogr.*, **14**, 649–655.